Made in United States of America
Reprinted from JOURNAL OF APPLIED METEOROLOGY
Vol. 36, No. 5, May 1997

Surface Radiative Fluxes in Sub-Sahel Africa

F. MISKOLCZI

Department of Meteorology, University of Maryland at College Park, College Park, Maryland

T. O. ARO AND M. IZIOMON

Department of Physics, University of Ilorin, Ilorin, Nigeria

R. T. PINKER

Department of Meteorology, University of Maryland at College Park, College Park, Maryland

(Manuscript received 19 January 1996, in final form 24 June 1996)

ABSTRACT

This paper reports results of observations of radiative fluxes measured in sub-Sahel Africa during a 2-yr period (1992–94). Shortwave radiation in the solar spectrum (0.2–4.0 μm), photosynthetically active radiation (0.4–0.7 μm), and longwave radiation (4.0–50.0 μm) were observed. In this study, the annual variability and the effects of dust on these fluxes (in particular, on the ratio of photosynthetically active radiation to the total shortwave radiation) were characterized. This ratio, known as the conversion factor, is important in modeling net primary productivity and the total CO_2 budget. In the past, this ratio was assumed to be constant. The authors' observations indicate that the daily average conversion factor has a strong annual cycle with a minimum of 0.41 in the middle of the dry season and a maximum of 0.55 in the first half of the rainy season, which is consistent with theoretical computations. The 2-yr mean is 0.49, only about 2% less than the nominal value of 0.50. The 2-yr mean values of the daily (24 h) averages of shortwave, photosynthetically active, and longwave downward fluxes are 200, 98, and 398 W m^{-2}, respectively. The average shortwave transmittance is 0.482. The two years of observations differed in the mean value of the downward shortwave component by about 7 W m^{-2}, the second year having lower values, with a similar decrease in photosynthetically active radiation and an increase in the longwave component by about 5 W m^{-2}, which would point to an increased cloudiness during the second year. The long-term objective of this study is to have high-quality ground truth in this climatic region for validating satellite-inferred surface radiative fluxes.

1. Introduction

Surface radiative fluxes play an important role in climate processes on all scales. The key elements involved in the exchange of energy between the surface and the atmosphere are the upwelling and downwelling shortwave (SW: 0.2–4.0 μm) and longwave (LW: 4.0–50.0 μm) fluxes. Photosynthetically active radiation (PAR: 0.4–0.7 μm) is known to play a key role in controlling CO_2 exchange (Bolin 1977; Daughtry et al. 1992), modeling of biological heating in oceans (Sathyendranath 1989), modeling of the hydrologic cycle by control of evapotranspiration (Sellers 1987), and modeling of biomass and crop yields (Daughtry et al. 1992; Kunkel 1990). Interest in PAR has recently increased because present global estimates of sources and sinks of CO_2 have been found not to balance; the increase of CO_2 in the atmosphere is less than that predicted from models that do not represent the feedback between the response of the biosphere and increased CO_2 (Kondratyev and Galindo 1994; Gifford 1994). According to the latter, the net primary productivity (NPP) of CO_2, namely, the rate of carbon assimilation, should increase by 10% if the anthropogenic emissions are to balance. This would require that the interactive contribution of biospheric dynamics to global climate change be modeled (Kondratyev and Grassl 1993).

Except for specific experiments in which direct measurements of PAR are made, PAR is usually estimated from the downwelling shortwave radiation using a nominal value of 0.5 for converting the total shortwave radiation to photosynthetically active radiation (Prentice et al. 1992; Running and Hunt 1993; Melillo et al. 1993). Model simulations have shown that the conversion factor (CF) depends on environmental conditions, such as clouds and aerosols (Pinker and Laszlo 1992). Ground observations on the variability of the CF are not con-

Corresponding author address: Dr. R. T. Pinker, Dept. of Meteorology, University of Maryland at College Park, 2213 Computer and Space Science Building, College Park, MD 20742.
E-mail: pinker@atmos.umd.edu

clusive. At some locations, no temporal variability in the CF has been observed (Howell et al. 1983). Satellite estimates of the CF do show spatial and temporal variability, but at some locations the temporal variability can be very small. Therefore, it is of interest to determine observationally the magnitude of the CF and, in particular, in regions of highly varying aerosols from natural sources. This requires simultaneous measurements of both PAR and SW radiation. Since SW radiation is more readily available than PAR, a better understanding of their relationship could lead to improvements in modeling NPP when information on only the total shortwave radiation is available. Optimally, direct knowledge of PAR, in addition to parameters that give information on the amount of available biomass [e.g., the normalized difference vegetation index (NDVI)], would be required inputs into models that predict NPP.

Very little is known on the variability of the downwelling longwave radiation in the sub-Sahel region. This is primarily due to problems related to the operation, maintenance, and interpretation of observations made with standard pyrgeometers (Philipona and Frohlich 1995). Information on this parameter is also of interest for modeling NPP because it determines the surface temperature, which is another key factor in the CO_2 exchange.

In this study, a pilot, long-term, observational effort was initiated in the fall of 1992 to observe selected radiative fluxes in the sub-Sahel, to learn about the annual variation of these parameters, and to build an infrastructure for future upgrading of local observational capabilities. It is anticipated that this location could become part of the Baseline Surface Radiation Network (BSRN) (WCRP-54 1991), aimed at monitoring radiative fluxes for detecting climate change and validating satellite-based retrieval methods of such fluxes. Moreover, the simultaneous operation of several instruments is helpful in the design of data quality control.

2. The site

The site selected for the observations of the surface radiative fluxes is located in sub-Sahel Africa on the campus of the University of Ilorin in Nigeria (8°32′N, 4°34′E), at an elevation of 350 m above sea level. It is positioned at the upper tip of the Guinea Savannah zone (Olaniran 1991), under the influence of the annual alternating southward and northward passage of the intertropical convergence zone (ITCZ). During the "dry season" (November–February), when the ITCZ appears slightly south or north of Ilorin, the prevailing northeasterly wind, known as the "harmattan," brings in air containing Saharan dust. The dust plumes originate from the Bodel Depression in the Chad Basin (Bertrand et al. 1979). During the harmattan, the atmospheric dust layer, which can have a thickness of up to 3 km, varies strongly in aerosol content, reducing the visibility to less than 1 km. During the "wet" season (March–October), conditions are typified by moist maritime southwesterly flow from the Gulf of Guinea. As such, this location is ideally suited for studying the effect of dust on surface radiative fluxes. Observations of aerosol optical depth at this site started in 1987 (Pinker et al. 1994) and are being continued.

3. Instruments and their calibration

The following instruments were deployed at the site: an Eppley precision spectral pyranometer (PSP, serial number 17675F3) for measuring the downwelling shortwave irradiance, an Eppley precision infrared radiometer (PIR, serial number 20468F3) for measuring the longwave irradiance, and a Li-Cor quantum sensor (serial number Q15183) for measuring the photosynthetic photon flux density (PPFD).

The PSP instrument was calibrated before deployment and at the end of a 2-yr measurement period. The calibration before deployment was done at the National Oceanic and Atmospheric Administration (NOAA) Air Resources Laboratory in Boulder, Colorado (J. DeLuisi 1992, personal communication). After two years of observations in Africa, the calibration was repeated at the World Radiation Center (WRC) in Davos, Switzerland (C. Frohlich and R. Philipona 1995, personal communication). In both cases, the PSP calibrations were performed by comparison with a reference standard instrument (whose calibration is traceable to a standard at Davos), using the sun and the sky as the source of radiation, under predominantly clear sky conditions. During the calibration period the measured SW downward flux varied between 340 and 670 W m^{-2}. At the Ilorin site, during the dusty, dry season and calm nights, a significant amount of dust deposits could accumulate on the dome. To maintain the accuracy of the calibration, daily cleaning of the dome was necessary. The calibration history of the instruments is given in Table 1. Based on these calibrations, updated calibration constants for every day were used in data reduction, as described in section 4.

The PIR was also calibrated before and after the measurement period, and during 13 November–7 December 1991 it participated in the BSRN broadband IR radiometer intercomparison at Coffeyville, Kansas. This field intercomparison showed that the instrument was operating according to its specifications for sensitivity, response time, and temperature dependance; namely, it did not show anomalous behavior compared to the other instruments (DeLuisi et al. 1992). After two years of use in Africa, the instrument was recalibrated at the WRC at Davos. The calibration history is presented in Table 1. Computation of longwave fluxes from the electrical signals measured by the instrument is more complex than for the shortwave fluxes and requires a theoretical–empirical approach. For several years now, the Albrecht and Cox (1977) approach has been widely accepted. To compute longwave fluxes with the Albrecht

TABLE 1. Calibration constants, dates, and location of calibrations for the instruments used.

Instrument	Date	Location	Calibration
Eppley PSP No. 17675F3 (μV W^{-1} m^2)	7 Oct 1994	Davos, WRC	8.55
	12 Dec 1991	Boulder, NOAA/ARL	8.69
	29 Aug 1984	Boulder, NOAA/ARL	8.92
	6 Oct 1978	Newport, Eppley Lab.	9.27
Eppley PIR No. 20468F3 (μV W^{-1} m^2)	7 Dec 1994	Davos, WRC	3.75
	29 Mar 1988	Newport, Eppley Lab.	3.92
	11 Dec 1980	Newport, Eppley Lab.	4.21
Licor LI190SA No. Q15183 (μA μE s m^2)	13 Jul 1995	Lincoln, LICOR Inc.	5.66
	23 Oct 1991	Lincoln, LICOR Inc.	6.70

ARL: Air Resources Laboratory, Boulder, Colorado.

and Cox (1977) formula requires knowledge of two parameters, known as the sensitivity factor C and the dome correction factor K. These are derived from calibration data and were provided to us by the calibration centers. In our estimation procedure of the longwave fluxes from the PIR measurements, an adjusted K factor was used, as will be explained in section 4. Additionally, we have used a newly proposed approach (Philipona and Frohlich 1995), which contains two additional correction parameters.

The quantum sensor was factory calibrated before deployment. At the end of the first two years, a new quantum sensor was purchased and factory calibrated. The field instrument was calibrated against the new instrument at Ilorin during an upgrade of the station in May 1995. This on-site calibration indicated a 30% degradation in the sensor's sensitivity. Subsequently, the instrument was returned to the factory and recalibrated under standard laboratory conditions. This latter calibration indicated a degradation of only 15%. The calibration history of the quantum sensor is also presented in Table 1.

The SW radiation is measured in units of watts per square meter, and PAR is measured in units of PPFD (μE s^{-1} m^{-2}). To compute the PAR conversion factor, the conversion of PPFD into watts per square meter is usually performed at the nominal wavelength of 0.485 μm. Selecting a slightly different wavelength for the conversion of the PPFD could change the value of the PAR conversion factor.

The data acquisition system was based on a CR10 Campbell Scientific data logger, which could operate on batteries for a reasonably long time. The thermopile voltages of the two Eppley instruments and the quantum sensor signal were measured in differential mode. The voltages of the pyrgeometer thermistors were measured using a dc half bridge with 800-mV excitation and 2-ms delay. To reduce the noise of the temperature measurements, two 28-kΩ series resistors were added to the body and dome thermistor circuitry. The thermistor resistance R_t was computed from the signal S using the following equation:

$$R_t = R_0(800.0 - S)S^{-1} - R_1, \quad (1)$$

where R_0 is the bridge resistor and R_1 is the series resistor. Temperatures were computed from the thermistor resistances by linear interpolation using the thermistor data sheets. Using the above arrangement the accuracy of the temperature measurements is limited only by the thermistor interchangeability, which is 0.1°C in the case of YSI 440031 thermistors. Data collection was programmed to a 1-s sampling rate and a 3-min integration time, in compliance with the World Climate Research Programme recommendations that time intervals be used that do not exceed 6 min and that divide the number 6 (Gilgen et al. 1995).

Every hour the temperature and the status of the CR10 internal battery were also measured. All data were stored in a storage module connected to the CR10. Once a week the storage module was downloaded to a personal computer. This system proved to be very efficient and supplied us with uninterrupted measurements for two years.

4. Measurements and computations

The measurements reported on in this paper cover a 2-yr period, beginning in September 1992 and ending in August 1994. To properly adjust the calibration of the instruments during the observational period, a linear regression between the calibration constants and the dates when they were performed was developed, as follows:

$$C = C_0 + C_1 d, \quad (2)$$

where C_0 and C_1 are the regression constants, and d is a variable defined by the algebraic sum of the actual year and the ratio of the day of the year to 365. Table 2 contains the regression constants used for adjusting the calibration of each instrument.

According to the theory of the thermopile-type radiation sensors, the sensitivity of such devices is inversely proportional to the third power of the absolute temperature of the cold junction. If the temperature of the cold junction is monitored, this decrease in sensitivity with increasing temperature can be corrected during the data-reduction process. Some instruments are

TABLE 2. The regression constants for Eq. (2), used for adjusting the calibration.

Instrument	C_0	C_1
PSP 17675F3 (μV W^{-1} m^2)	94.47632	−0.04307789
PIR 20468F3 (μV W^{-1} m^2)	69.53616	−0.032985332
Q15183 (μE s^{-1} m^{-2} mV^{-1})	−32 614.11	16.4911

supplied with a thermistor–resistor temperature compensation circuit to adjust the output signal properly to the sensitivity determined by the actual cold junction temperature. The PSP as well as the PIR instruments are temperature compensated, but according to the factory calibration a 2% temperature dependence still remains. This dependence was eliminated using a correction factor r for both the pyranometer and the pyrgeometer, expressed as a function of the measured pyrgeometer case temperature T_c (°C), as follows:

$$r = 0.99843 + T_c(4.54761 \times 10^{-4} - 5.23809 \times 10^{-6}T_c). \quad (3)$$

Every 3 min, the daily updated calibration factors of the PSP and PIR were multiplied by r. The numerical constants in Eq. (3) were obtained by a second-order regression scheme applied to the temperature-dependent curve of the relative sensitivity in the instrument's factory calibration sheet. No temperature correction was introduced to the calibration of the quantum sensor.

The PIR was neither shaded nor ventilated. Because of dome heating, there could be anomalous behavior in the longwave radiation, which can be seen in the high-resolution 3-min averages as a correlation between the shortwave and longwave fluxes (Fig. 1). Such correlation is not evident in data averaged over longer periods of time (e.g., 1 h). In order to eliminate such effects, the following procedure was followed. For each day, using the 3-min averages, a covariance matrix between the shortwave and the longwave flux components and the pyrgeometer case temperature was computed. The dome heating constant K was adjusted in such a way that the correlation between the SW and LW radiation was kept at the same level that exists between the SW and σT_c^4, where σ is the Stefan–Boltzmann constant and T_c is the case absolute temperature. This procedure was repeated with the SW and LW 3-min data for each day, and a new K coefficient was obtained and used with the Albrecht and Cox (1977) formula, given as

$$\mathrm{LW} = CP + \sigma T_c^4 - K\sigma(T_d^4 - T_c^4), \quad (4)$$

where C (W m^{-2} mV^{-1}) is a calibration constant, P is the thermopile voltage, T_d are the dome absolute temperatures, and K is the dome heating constant.

To improve the computations of LW radiation from the observed pyrgeometer signals, Philipona and Frohlich (1995) recommend the use of the following formula:

$$\mathrm{LW} = CP(1 + K_1\sigma T_c^3)^{-1} + K_2\sigma T_c^4 - K\sigma(T_d^4 - T_c^4), \quad (5)$$

where K_1 and K_2 are newly introduced correction factors. The calibration of the PIR at the end of the 2-yr observational period in Nigeria was done in the blackbody radiation source of the WRC at Davos. The required parameters (C, K, K_1, and K_2) of Eqs. (4) and (5) were determined from the same calibration measurements. Body and dome temperatures were determined using the Steinhart and Hart equation and the standard YSI coefficients of the YSI 44031 thermistors. The modifications in the pyrgeometer circuitry were accounted for in the calibration procedure. The pyrgeometer calibration parameters are summarized in Table 3.

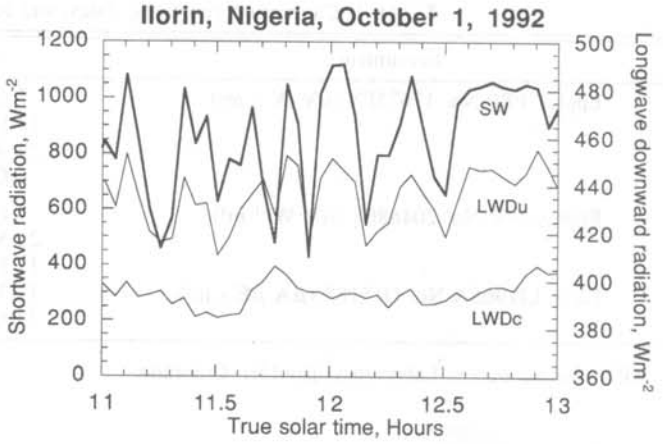

FIG. 1. The temporal variation of 3-min-averaged shortwave (SW) uncorrected downward longwave (LWDu) and corrected downward longwave (LWDc) radiative fluxes at Ilorin on 1 October 1992, starting at 1100 true solar time. Illustrated are the effects of dome heating by solar radiation on the measured downward longwave radiation.

To assess the potential differences in the computed LW radiative fluxes due to different reduction formulas used, the LW fluxes were derived with both formulas for September 1992, using 3-min-averaged observations. The results are presented in Table 4. As evident, the average difference is less than 4 W m^{-2}. For the evaluation of the 2-yr record of LW radiation, Eq. (4) was used.

In Fig. 1, the temporal variation of the 3-min-averaged SW and LW downward radiative fluxes on 1 October 1992, starting at 1100 true solar time, is presented.

TABLE 3. Pyrgeometer calibration parameters.

Calibration parameters	Method of computation: Albrecht–Cox, Eq. (4)	Method of computation: Philippona–Frohlich, Eq. (5)
C (μV W^{-1} m^2)	3.75	4.47
K	3.65	3.54
K_1	—	0.0923
K_2	—	0.9904

TABLE 4. Longwave downward irradiance (W m^{-2}) at Ilorin, as computed with the Albrecht–Cox and Philipona–Frohlich formulas for November 1993 (14 400 3-min-averaged observations).

Statistics	Method of computation	
	Albrecht–Cox	Philipona–Frohlich
Minimum	352.08	356.15
Maximum	447.69	452.89
Average	398.72	402.79
Std. dev.	15.43	15.43

The effect of dome heating by solar radiation on the measured LW radiation is evident (LWDu and LWDc are the uncorrected and corrected longwave downward fluxes). In this case, the dome heating constant was 4.75, which is 30% higher than the nominal value of 3.65, resulting in about 15 W m^{-2} increase in the dome correction term in Eq. (4). At noon (11.8° zenith angle), when the magnitude of the global solar radiation was 1100 W m^{-2}, the magnitude of the dome correction term was 57 W m^{-2}. This value is almost double that of the dome correction term that was obtained by Culf and Gash (1993) in Niger, using a regression equation derived by using sun shading method.

The conversion factor was computed for every 3-min interval, and subsequently a daily average was derived. To ensure high quality of observations and to eliminate spurious errors that could arise by incidental shading of an instrument, all observations for which the SW radiation was less than 20 W m^{-2} and PAR was less than 10 W m^{-2} were eliminated. The standard deviations σ of the 3-min values were also computed on a daily basis. Observations that were outside a 3σ interval were excluded. Furthermore, because of the cosine response of the quantum sensor, no measurements made at solar zenith angles larger than 80° were included in the computations of the CF.

TABLE 6. Basic statistics for the histograms of the SW components in Figs. 2 and 4; radiative terms are in watts per square meter.

Statistics	Daytime (N = 174 844)			Daytime (N = 151 241)	
	EXT	SW	PAR	CF′	TR
Minimum	0	0	0	0.37	0.02
Maximum	1373	1370	676	0.76	1.03
Average	827	397	195	0.496	0.459
Median	919	354	176	0.49	0.47
Std. dev.	405	296	143	0.03	0.19

CF: PAR conversion factor computed from the 3-min averages.
TR: Shortwave flux transmittance (SW/EXT).
N: Number of cases.

5. Results and discussion

In Table 5 the basic statistics for the daily averages of the observed parameters are presented for each year and for the entire 2-yr measurement period. In Tables 6 and 7 the statistics for the 3-min averages of the measured parameters are given separately for daytime and nighttime observations.

In Fig. 2 we present the temporal variability in the daily average values of the extraterrestrial (EXT), surface downwelling SW, and PAR radiation, as well as the shortwave atmospheric transmittance (TR), for the entire 2-yr observational period that started on 1 September 1992. The TR was computed as the ratio of the surface measured value to the extraterrestrial value. The surface observations of both the SW and PAR radiation are strongly forced by the extraterrestrial radiation, es-

TABLE 5. Basic statistics for the daily averages of observed parameters. Radiative terms are in watts per square meter, and T_c is in degrees Celsius.

Time period	Statistics	Observed parameters							
		EXT	SW	PAR	CF	LW	Pile	DC	T_c
First-year daily averages	Minimum	370	49.7	26.0	0.440	334	−132	−0.2	20.4
	Maximum	441	295	150	0.550	424	−12	12	32.4
	Average	415	203	101	0.497	395	−59	8.4	27.1
	Median	425	209	103	0.500	402	−53	8.7	27.0
	Std. dev.	23.0	44.3	22.3	0.020	21.7	24.9	1.9	2.2
Second-year daily averages	Minimum	370	54.6	26.2	0.410	343	−103	2.3	21.5
	Maximum	441	284	141	0.530	427	−15	13	32.4
	Average	415	197	95	0.483	400	−54	8.5	27.3
	Median	425	199	96	0.490	405	−51	8.5	27.3
	Std. dev.	22.9	43.4	22.5	0.020	15.5	19.3	2.0	2.3
2-yr daily averages	Minimum	370	49.7	26.0	0.410	334	−132	−0.2	20.4
	Maximum	441	295	150	0.550	427	−13	13	32.4
	Average	415	200	98	0.490	398	−56	8.5	27.2
	Median	425	204	99	0.490	403	−52	8.7	27.1
	Std. dev.	22.9	44.0	22.6	0.020	19.0	22.4	2.0	2.2

EXT: Extraterrestrial solar radiation computed using 1372 W m^{-2} as the solar constant.
DC: Dome correction term.
Pile: Thermopile output of the PIR pyrgeometer.

TABLE 7. Basic statistics for the histograms of the longwave components in Figs. 9 and 10. Radiative terms are in watts per square meter, and T_c is in degrees Celsius.

	Daytime (174 844 data points)				Nighttime (171 645 data points)			
Statistics	LW	Pile	DC	T_c	LW	Pile	DC	T_c
Minimum	306	−185	−25.8	14.6	309	−155	−7.3	14.7
Maximum	465	19.5	58.2	43.5	455	11.0	7.7	36.6
Average	403	−62.8	15.9	30.4	392	−49.8	1.1	24.1
Median	408	−61.9	13.5	30.8	394	−53.0	1.1	23.5
Std. dev.	23.3	35.5	12.4	5.7	24.9	28.7	1.2	3.1

pecially during the dry season. There is a slightly negative trend during the two years, resulting in 6.70 and 5.75 W m^{-2} yr^{-1} differences in the annual mean of daily averages of SW and PAR radiation, respectively. The temporal variability in the TR also shows a negative trend, which is consistent with the trend in the SW and PAR. In Fig. 3 we present the frequency distribution of the 3-min averages of extraterrestrial and measured surface SW radiation for a 2-yr period (Fig. 3a), and similar results for PAR (Fig. 3b) and for the shortwave atmospheric transmittance (Fig. 3c). These results illustrate the strong effects of clouds on the distribution of the surface SW and PAR fluxes. In Fig. 3c it is shown that in 75% of the cases the transmittance was between 0.20 and 0.70, and only in about 2% of the cases it exceeded 0.80.

In Fig. 4 it is shown that there is a strong seasonal variability in the conversion factor. The computations presented in this figure were performed once using the daily average PAR (solid line) and once using the 3-min average values (dots). In reality, plants respond to the instantaneous value of PAR. Therefore, the variability in the conversion factor on shorter timescales might be more appropriate for use than values that are reported from observations that are time averaged. The frequency distribution of the 3-min-averaged CF is presented in Fig. 5. As is evident, 90% of the cases are found to be between 0.43 and 0.55. Based on data presented in Tables 5 and 6, the minimal values of the conversion factors computed from the daily and the 3-min averages are about 0.41 and 0.37, respectively, and they occur during the dry season. The highest values are 0.55 and 0.76, respectively, and they occur during the rainy season. The observed annual variability of the CF is due to the combined effects of water vapor and aerosols. In

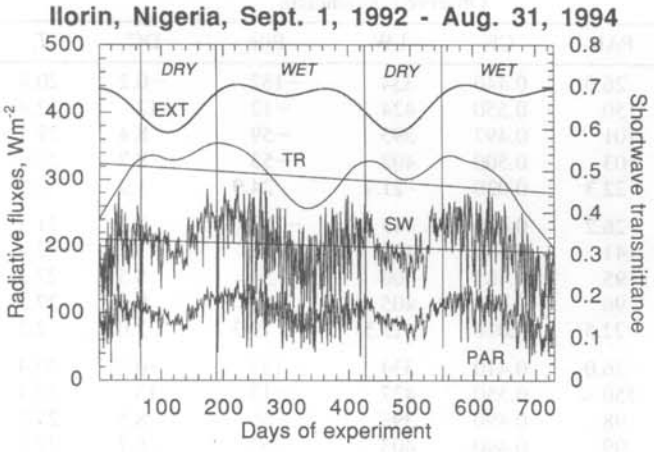

FIG. 2. The temporal variation of the daily average values of extraterrestrial (EXT) surface shortwave (SW) shortwave transmittance (TR) and (PAR) radiation at Ilorin for a 2-yr period starting 1 September 1992. Trends in the (SW) and (TR) are also displayed, as well as the duration of the dry and wet seasons.

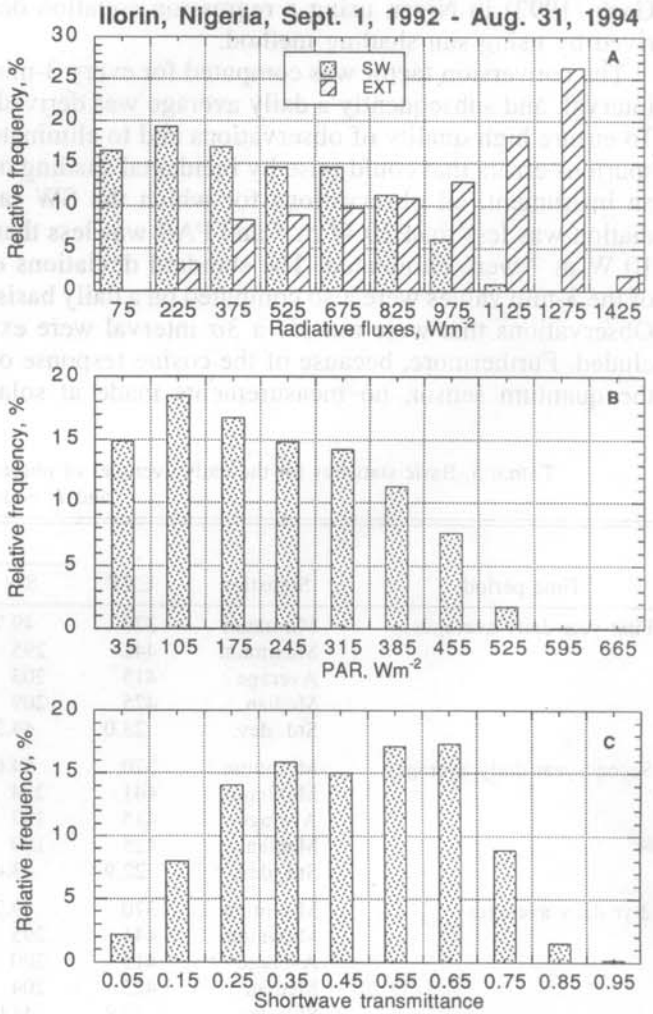

FIG. 3. (a) Frequency distribution of 3-min averages of extraterrestrial and measured surface (SW) radiation at Ilorin for a 2-yr period, starting 1 September 1992. (b) Same as (a) but for the measured (PAR). (c) Same as (a) but for the shortwave transmittance.

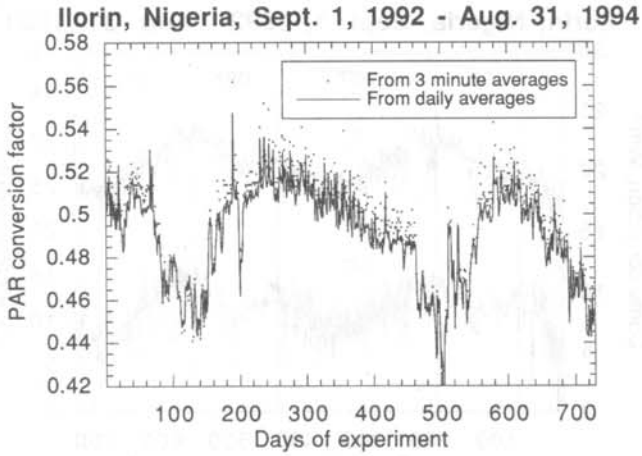

FIG. 4. The temporal variation of the conversion factor at Ilorin for a 2-yr period starting 1 September 1992. The computations were performed once using the daily average (PAR) (solid line) and once using the 3-min average values (dots).

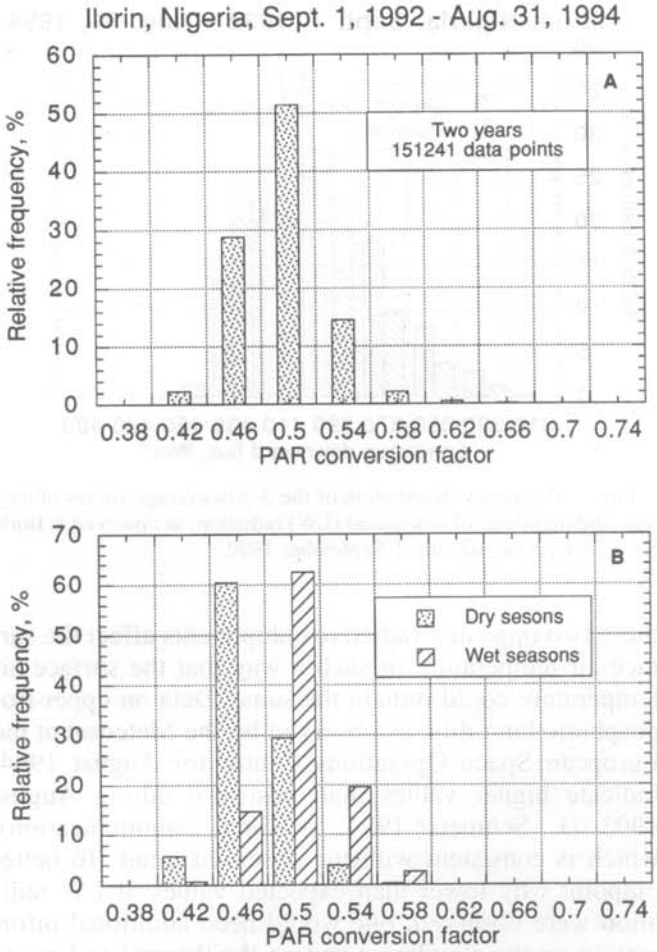

FIG. 5. (a) Frequency distribution of the 3-min average values of the conversion factor, as observed at Ilorin for a 2-yr period starting 1 September 1992. (b) Same as (a) but separated for the dry and wet seasons.

the wet season, the increased water vapor absorption in the near-infrared region decreases the total SW flux, while not much affecting the PAR. The net result is a larger conversion factor. During the dry seasons, according to Fig. 2, the shortwave transmittance increased significantly. This is partly due to the reduced water vapor absorption in the near-infrared region. In the PAR spectral region the radiation is lower due to increased absorption from the longer optical path, which is in turn due to the increased scattering at higher dust and aerosol loading of the atmosphere. Both effects tend to decrease the PAR conversion factor.

In Fig. 6 we present the temporal variability in the downward LW radiation as computed by the Albrecht and Cox (1977) formula. The minimum occurs during the harmattan due to the combined effect of colder air temperatures resulting from the lower extraterrestrial SW forcing and the higher transparency due to less cloudiness. The magnitude of the minimum is probably moderated by the greenhouse effect of the harmattan dust. Based on the two years of observations, the annual average LW irradiance is 398 W m^{-2} (Table 5). This value is very close to the computed value of 396 W m^{-2} for the LOWTRAN 7 tropical model atmosphere and for clear-sky conditions. The average surface temperature measured at Ilorin under all-sky conditions is higher by about 0.7°C than the LOWTRAN 7 clear-sky tropical model atmosphere. Under the all-sky conditions that existed at Ilorin, one would expect larger LW irradiance. Possibly, the LOWTRAN 7 tropical model atmosphere is not appropriate for this geographical location of the sub-Sahel. In Fig. 6 the temporal variability of the ambient air temperature as approximated by the pyrgeometer case temperature is also shown. As evident, there was an increase in the downward component of the LW radiation during the 2-yr period, while the surface air temperature was almost unchanged. These findings and those presented in Fig. 2 would indicate that there might have been an increase in cloudiness or humidity (or both) during the second year, which would reduce the SW and increase the LW radiation. From the point of view of climate stability, it is interesting to note that

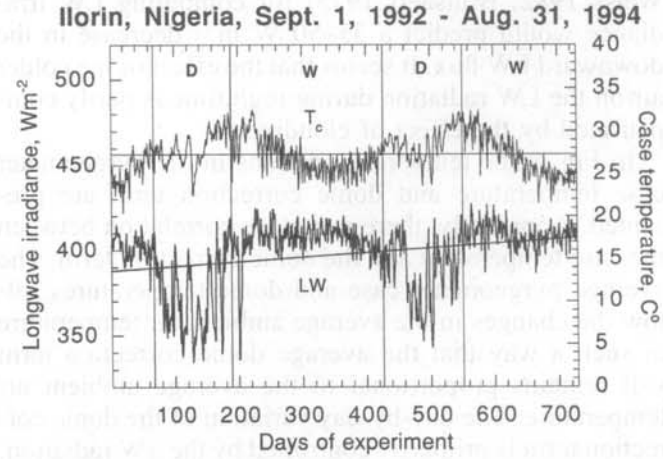

FIG. 6. The temporal variation of the daily average values of downward surface (LW) radiation and the pyrgeometer case temperature T_c at Ilorin for a 2-yr period starting 1 September 1992.

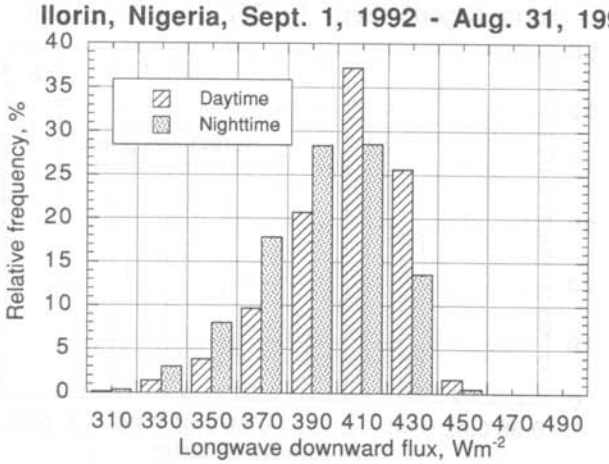

FIG. 7. Frequency distribution of the 3-min average values of daytime and nighttime of downward (LW) radiation, as observed at Ilorin for a 2-yr period starting 1 September 1992.

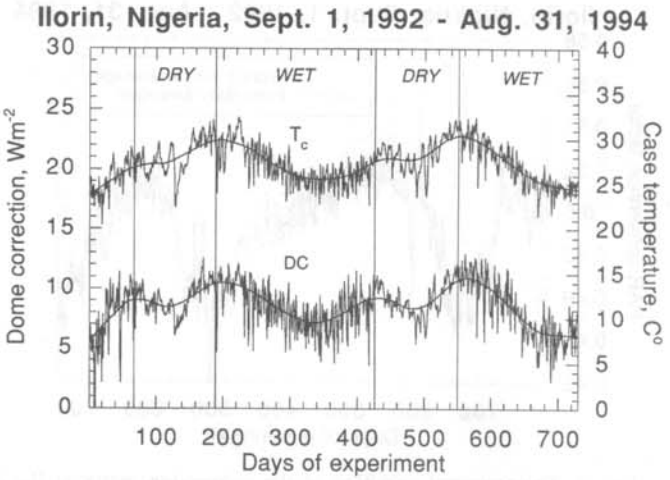

FIG. 8. Temporal variation of the (PIR) case temperature T_c and the corresponding dome correction (DC) at Ilorin for a 2-yr period starting 1 September 1992. A 50-day running mean filter was applied, as illustrated.

these two opposing radiative components affect the surface air temperature in such a way that the surface air temperature could remain the same. Data on upper-tropospheric humidity, as observed by the Meteosat at the European Space Operations Centre for August 1994, indicate higher values than observed during August 1993 (J. Schmetz 1994, personal communication), which is consistent with the observed trend. To better pinpoint why lower than expected values of LW radiation were observed, one would need additional information on the cloudiness and on the thermal and moisture structure of the atmosphere.

In Fig. 7 the frequency distribution of the 3-min-averaged daytime and nighttime values of LW radiation for the 2-yr period is presented. As expected, the daytime LW fluxes are larger than the nighttime fluxes, but their overall difference for the whole measurement period is only 11 W m^{-2}. Considering the differences in the corresponding T_c values in Table 7, this difference is surprisingly small. For such a decrease in the ambient air temperature, the common empirical formulas (e.g., Weiss 1982; Brutsaert 1975) for computing LW irradiance would predict a 35–50 W m^{-2} decrease in the downward LW flux. It seems that the effect of the colder air on the LW radiation during nighttime is partly compensated by the effect of cloudiness.

In Fig. 8 the temporal variations in the pyrgeometer case temperature and dome correction term are presented. Apparently, there is a close correlation between the case temperature and the dome correction term. The average pyrgeometer case and dome temperatures follow the changes in the average ambient air temperature in such a way that the average dome correction term still remains proportional to the average ambient air temperature. The day-by-day variation of the dome correction term is primarily controlled by the SW radiation. Using the high-resolution 3-min data, the amplitude in the dome correction term can be as high as 58.2 W m^{-2} (Table 7). In some cases, when the overheated dome is exposed to the onset of rain, large negative dome correction terms are measured with a minimum value of -25.8 W m^{-2}. Figures 9a–c show the frequency distribution of the pyrgeometer case temperature, dome correction term, and pile contribution, respectively.

In Fig. 10 details on the diurnal variability of the PAR conversion factor are presented. The monthly average diurnal variations of CF, presented for each month, show consistent behavior. The CF increases with increasing air mass over the course of the day. The magnitude of the increase is apparently larger in the afternoon, which may be related to the diurnal cycle of the humidity during the rainy season and to the diurnal cycle of the dust loading of the atmosphere during the dry harmattan. To quantify this relationship, regular radiosonde, surface humidity, and turbidity measurements are required. The separation of the monthly diurnal curves is also consistent with the seasonal variation of the CF, as presented in Fig. 4. The slight local maximum in the morning at around 0900 in each month can be attributed to the imperfect cosine response of the quantum sensor. This effect may be masked out in the afternoon by the sharper increase of the curves.

6. Summary

This paper presents results from a relatively long-term, uninterrupted record of observations of radiative fluxes in a sub-Sahel region of Africa. The high-frequency observations were averaged over 3-min time intervals, and as such, they are suitable for a wide range of investigations. Statistics from this high-resolution record gave us a valuable insight into the range and temporal variability of radiative flux components, CF, and SW transparency of the tropical atmosphere. Moreover, the high-frequency observations allowed the removal of solar influences from the LW fluxes, which is not possible when hourly averaged data are used. There-

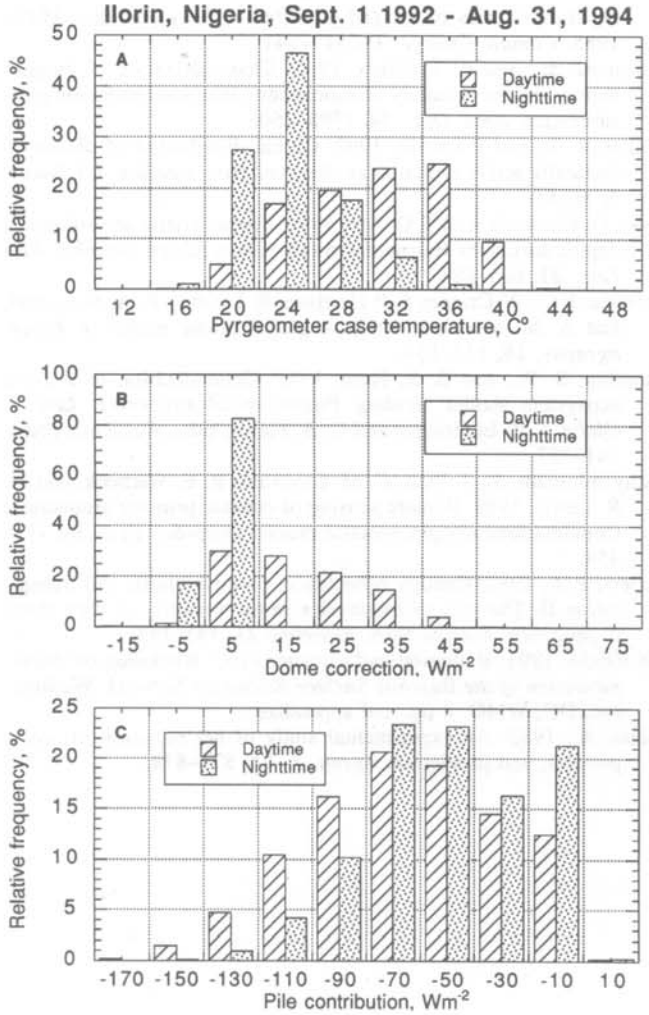

FIG. 9. Frequency distribution of the 3-min average daytime and nighttime values of (a) PIR case temperature, (b) dome correction, and (c) pile contribution.

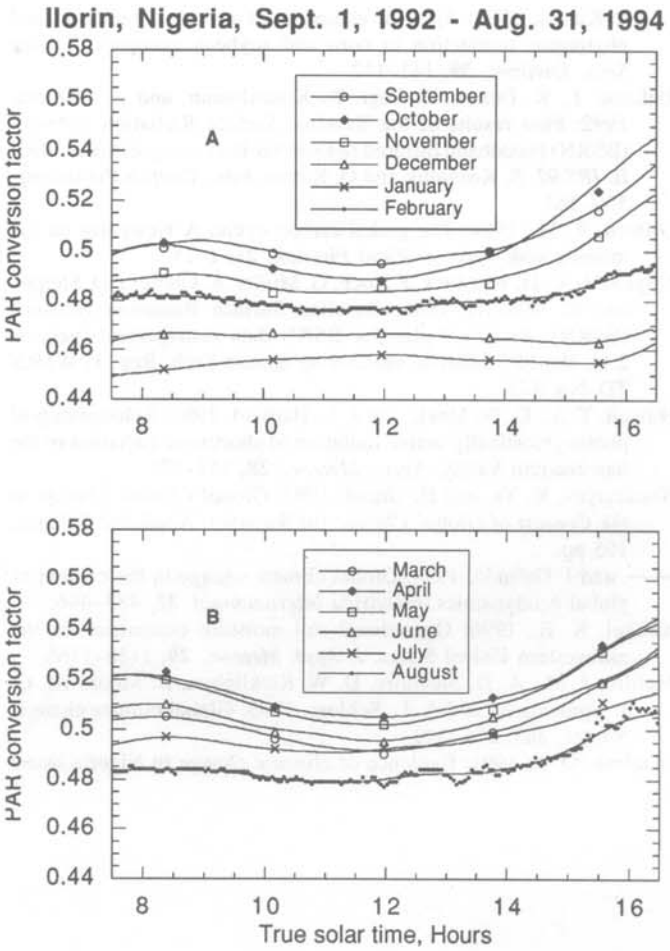

FIG. 10. Two-year-averaged monthly mean diurnal variation of the conversion factor at Ilorin starting 1 September 1992.

fore, the LW observations reported in this study are unique for the African continent. Comparisons of our LW observations with modeled values based on the standard profiles for this region indicate that these latter profiles might not be representative of the sub-Sahel environment. We have also detected a clear signal of dust effects on the conversion factor of a magnitude that is significant in CO_2 modeling. The long-term objective of this activity is to use these observations to validate and improve satellite estimates of surface radiation fluxes, known to be affected by aerosols, particularly in regions under the influence of severe dust outbreaks. The measured original high-resolution radiation data are archived at the Geographisches Institut in Zurich, Switzerland, at the University of Ilorin, and at the University of Maryland, College Park, in College Park, Maryland. Further activity to upgrade the Ilorin station to facilitate the operational measurements of diffuse and direct radiation components, spectral turbidity, ambient air temperature, relative humidity, and rain events is in progress.

Acknowledgments. This work was supported by Grant NA36GP0386 from the NOAA Climate and Global Change Program, Grant NSFD-INT-9015324 from Operational Measurements, and a travel grant from the World Climate and Research Program of the World Meteorological Organization (WMO). Thanks are due to the granting agencies; to Dr. R. Newson from the Joint Planning Staff of the WMO for his support; to Drs. A. Ohmura, J. DeLuisi, C. Frohlich, and R. Philipona for help with the calibration of the instruments; and to the Senate Research Grant Committee, University of Ilorin.

REFERENCES

Albrecht, B., and S. K. Cox, 1977: Procedures for improving pyrgeometer performance. *J. Appl. Meteor.*, **16,** 188–197.

Bertrand, J., A. Cerf, and J. K. Domergue, 1979: Repartition in space and time of dust haze south of the Sahara. *W. M. D.*, **538,** 409–415.

Bolin, B., 1977: Changes of land biota and their importance for the carbon cycle. *Science,* **196,** 613–615.

Brutsaert, W., 1975: On a derivable formula for longwave radiation from clear skies. *Water Resour. Res.,* **11,** 742–744.

Culf, A. D., and J. H. C. Gash, 1993: Longwave radiation from clear skies in Niger: A comparison of observations with simple formulas. *J. Appl. Meteor.*, **32,** 539–547.

Daughtry, C. S. T., K. P. Gallo, S. N. Goward, S. D. Prince, and W.

P. Kustas, 1992: Spectral estimates of absorbed radiation and phytomass production in corn and soybean canopies. *Remote Sens. Environ.,* **39,** 141–152.

DeLuisi, J., K. Dehne, R. Vogt, K. Konzelmann, and A. Ohmura, 1992: First results of the Baseline Surface Radiation Network (BSRN) broadband infrared radiometer inter comparison at FIRE II. *IRS 92,* S. Keevallik and O. Karner, Eds., Deepak Publishing, 559–564.

Gifford, R. M., 1994: The global carbon cycle: A viewpoint on the missing sink. *Aust. J. Plant Physiol.,* **21,** 1–15.

Gilgen, H., C. H. Whitlock, F. Koch, G. Muller, A. Ohmura, D. Steiger, and R. Wheeler, 1995: Baseline Surface Radiation Network (BSRN): Technical plan for BSRN data management (version 2.1). World Radiation Monitoring Centre Tech. Rep. 1, WMO/TD–No. 443.

Howell, T. A., D. W. Meek, and J. L. Hatfield, 1983: Relationship of photosynthetically active radiation to shortwave radiation in the San Joaquin Valley. *Agric. Meteor.,* **28,** 157–175.

Kondratyev, K. Ya, and H. Grassl, 1993: *Global Climate Change in the Context of Global Change* (in Russian). Academic Science, 195 pp.

——, and I. Galindo, 1994: Global climate change in the context of global ecodynamics. *Geofisica Internacional,* **33,** 487–496.

Kunkel, K. E., 1990: Operational soil moisture estimation for the midwestern United States. *J. Appl. Meteor.,* **29,** 1158–1166.

Melillo, J. M., A. D. McGuire, D. W. Kicklighter, B. Moore III, C. J. Vorosmarty, and A. L. Schloss, 1993: Global climate change. *Nature,* **363,** 234–240.

Olaniran, O. J., 1991: Evidence of climatic change in Nigeria based on annual series of rainfall of different daily amounts, 1949–1985. *Climate Change,* **19,** 319–341.

Philipona, R., and C. Frohlich, 1995: Characterization of pyrgeometers and the accuracy of atmospheric longwave radiation measurements. *Appl. Opt.,* **34,** 1598–1605.

Pinker, R. T., and I. Laszlo, 1992: Global distribution of photosynthetically active radiation as observed from satellite. *J. Climate,* **5,** 56–65.

——, G. Idemudia, and T. O. Aro, 1994: Characteristic aerosoloptical depths during the Harmattan in sub-Sahara Africa. *Geophys. Res. Lett.,* **21,** 685–688.

Prentice, I. C., W. Cramer, S. P. Harrison, R. Leemas, R. A. Monserud, and A. M. Solomon, 1992: A global biome model. *J. Biogeography,* **19,** 117–134.

Running, S. W., and E. R. Hunt, 1993: Generalization of a forest ecosystem model. *Scaling Physiological Processes: Leaf to Globe,* J. R. Ehleringer and C. B. Fields, Eds., Academic Press, 141–157.

Sathyendranath, S., T. Platt, C. M. Caverhill, R. E. Warnock, and M. R. Lewis, 1989: Remote sensing of oceanic primary production: Computations using a spectral model. *Deep-Sea Res.,* **36,** 431–454.

Sellers, P. J., 1987: Canopy reflectance, photosynthesis and transpiration II. The role of biophysics in the linearity of their interdependence. *Remote Sens. Environ.,* **21,** 143–183.

WCRP-54, 1991: Radiation and climate. *Proc. Workshop on implementation of the Baseline Surface Radiation Network.* Washington, DC, WMO, 8 pp. and appendixes.

Weiss, A., 1982: An experimental study of net radiation, its components, and prediction. *Agron. J.,* **74,** 871–874.